



1 **Exclusively heteronuclear NMR experiments for the investigation of intrinsically disordered**  
2 **proteins: focusing on proline residues**

3

4 Isabella C. Felli<sup>1</sup>, Wolfgang Bermel<sup>2</sup> and Roberta Pierattelli<sup>1</sup>

5

6 <sup>1</sup>CERM Department of Chemistry “Ugo Schiff”, University of Florence, Via Luigi Sacconi 6, 50019 Sesto  
7 Fiorentino, Florence, Italy

8 <sup>2</sup>Bruker BioSpin GmbH, Silberstreifen, 76287 Rheinstetten, Germany

9

10 *Corresponce to:*

11 Isabella C. Felli ([felli@cerm.unifi.it](mailto:felli@cerm.unifi.it)) and Roberta Pierattelli ([roberta.pierattelli@unifi.it](mailto:roberta.pierattelli@unifi.it))

12

13 **Keywords**

14 <sup>13</sup>C detection, IDP, NMR

15

16 **Abstract**

17 NMR represents a key spectroscopic technique to contribute to the emerging field of highly flexible,  
18 intrinsically disordered proteins (IDPs) or protein regions (IDRs) that lack a stable three-dimensional  
19 structure. A set of exclusively heteronuclear NMR experiments tailored for proline residues, highly  
20 abundant in IDPs/IDRs, are presented here. They provide a valuable complement to the widely used  
21 approach based on amide proton detection, filling the gap introduced by the lack of amide protons in  
22 prolines within polypeptide chains. The novel experiments have very interesting properties for the  
23 investigations of IDPs/IDRs of increasing complexity.

24

25



## 26 Introduction

27 Invisible in X-ray studies of protein crystals, intrinsically disordered regions (IDRs) of complex proteins  
28 have been for a long time considered just passive linkers connecting functional globular domains and thus  
29 often ignored in structural biology studies. However, in many cases they comprise a significant fraction of  
30 the primary sequence of a protein and for this reason they are expected to have a role in protein function  
31 (Van Der Lee et al., 2014). The characterization of highly flexible regions of large proteins as well as entire  
32 proteins characterized by the lack of a 3D structure, now generally referred to as intrinsically disordered  
33 proteins (IDPs), lies well behind that of their folded counterparts and is nowadays pursued by an  
34 increasingly large number of studies to fill this knowledge gap. NMR plays a strategic role in this context  
35 since it constitutes the major, if not the unique, spectroscopic technique to achieve atomic resolution  
36 information on their structural and dynamic properties. However, intrinsic disorder and high flexibility  
37 have very relevant effects for NMR investigations such as reduction of chemical shift dispersion as well as  
38 efficient exchange processes with the solvent due to the open conformations that, when approaching  
39 physiological pH and temperature, broaden amide proton resonances beyond detection. While several  
40 elegant experiments were proposed to exploit exchange processes with the solvent (Kurzbaach et al., 2017;  
41 Olsen et al., 2020; Szekely et al., 2018; Thakur et al., 2013), in general initial NMR investigations of  
42 IDPs/IDRs are carried out in conditions in which these critical points are mitigated. Exchange broadening  
43 strongly depends on pH and temperature; conditions can be optimized to recover most of the amide  
44 proton resonances enabling the acquisition of amide proton detected triple resonance experiments  
45 needed for sequence-specific assignment of the resonances. However, in particular for proteins that are  
46 largely exposed to the solvent it may be interesting to study them near physiological pH and temperature  
47 conditions (Gil et al., 2013). In this context,  $^{13}\text{C}$  direct detection NMR developed into a valuable alternative.  
48 Although the intrinsic sensitivity of  $^{13}\text{C}$  is lower with respect to that of  $^1\text{H}$ ,  $^{13}\text{C}$  nuclear spins are  
49 characterized by a large chemical shift dispersion (Dyson, H. Jane; Wright, 2001) and, when coupled to  $^{15}\text{N}$   
50 nuclei, provide a well-defined fingerprint of a polypeptide (Bermel et al., 2006a; Hsu et al., 2009; Lopez et  
51 al., 2016; Schiavina et al., 2019). These features were exploited to design a suite of 3D experiments based  
52 on carbonyl-carbon direct detection for sequential assignment and to measure NMR observables (Felli  
53 and Pierattelli, 2014). These experiments exploit only heteronuclear chemical shifts in the indirect  
54 dimensions to maximize chemical shift dispersion (exclusively heteronuclear experiments) and can be  
55 used to study IDPs/IDRs also in conditions in which amide proton resonances are too broad to be detected.  
56 In addition, they reveal information about proline residues that lack the amide proton when part of



57 polypeptide chains and cannot be detected in 2D HN correlation experiments even if pH and temperature  
58 conditions are optimized to reduce exchange broadening.

59 Proline residues are abundant in IDPs/IDRs and often occur in proline-rich sequences with repetitive units  
60 (Theillet et al., 2014). Initial bioinformatics studies on the relative abundance of each amino acid in regions  
61 of the protein that could not be observed in X-ray diffraction studies led to the classification of prolines  
62 as “disorder promoting” amino acids (Dunker et al., 2008). Nevertheless proline, the only imino acid,  
63 features a closed ring in its side chain which confers local rigidity compared to all other amino acids  
64 (Williamson, 1994), as also exploited in FRET studies in which proline residues are used as rigid spacers to  
65 measure distances (Schuler et al., 2005). These observations clearly show the importance of experimental  
66 atomic resolution information on the structural and dynamic properties of proline residues to understand  
67 their role in modulating protein function. While abundant information about proline residues in globular  
68 protein folds is available either through NMR or X-ray studies (MacArthur and Thornton, 1991), including  
69 several examples of cis-trans isomerization of peptide bonds involving proline nitrogen as molecular  
70 switches (Lu et al., 2007), their characterization in highly flexible, disordered polypeptides is available only  
71 in a handful of cases (Chaves-Arquero et al., 2018; Gibbs et al., 2017; Haba et al., 2013; Hošek et al., 2016;  
72 Knoblich et al., 2009; Pérez et al., 2009; Piai et al., 2016) and actually early studies on IDPs/IDRs routinely  
73 reported assignment statistics only considering all other amino acids (“excluding prolines”).

74 Here we would like to propose an experimental variant of the most widely used  $^{13}\text{C}$  detected 3D  
75 experiments for sequence-specific assignment of IDPs/IDRs to selectively pick up correlations involving  
76 proline nitrogen nuclei and provide key complementary information to that obtained through amide  
77 proton detected experiments. They can be collected in a shorter time with respect to standard 3D  
78 experiments and provide a valuable addition to the current experimental protocols for the study of IDPs.

79

## 80 **Materials and methods**

81 Isotopically labelled  $\alpha$ -synuclein ( $^{13}\text{C}$  and  $^{15}\text{N}$ ) was expressed and purified as previously described (Huang  
82 et al., 2005). The NMR sample has 0.6 mM protein concentration in 20 mM phosphate buffer at pH 6.5  
83 and 100 mM NaCl in  $\text{H}_2\text{O}$  with 5%  $\text{D}_2\text{O}$  for the lock signal.

84 Isotopically labelled CBP-ID4 ( $^{13}\text{C}$  and  $^{15}\text{N}$ ) was expressed and purified as previously described (Piai et al.,  
85 2016). The NMR sample has 0.9 mM protein concentration in water buffer containing 20 mM TRIS, 50 mM  
86 KCl, at pH 6.9, with 5%  $\text{D}_2\text{O}$  added for the lock signal.



87 NMR experiments were acquired at 288 K (for  $\alpha$ -synuclein) and at 283K (for CBP-ID4) with a 16.4 T Bruker  
88 AVANCE NEO spectrometer operating at 700.06 MHz  $^1\text{H}$ , 176.05 MHz  $^{13}\text{C}$ , and 70.97 MHz  $^{15}\text{N}$  frequencies,  
89 equipped with a 5 mm cryogenically cooled probehead optimized for  $^{13}\text{C}$  direct detection (TXO). RF pulses  
90 and carrier frequencies typically employed for the investigation of intrinsically disordered proteins were  
91 used, except for the modifications introduced to zoom into the proline  $^{15}\text{N}$  region. Carrier frequencies  
92 were set to 4.7 ppm ( $^1\text{H}$ ), 176.4 ( $^{13}\text{C}$ ), 53.9 ( $^{13}\text{C}^\alpha$ ), 44.9 ( $^{13}\text{C}^{\text{all}}$ ); the  $^{15}\text{N}$  carrier was set to 137 ppm, in the  
93 center of  $^{15}\text{N}$  resonances of proline residues. Hard pulses were used for  $^1\text{H}$ . Band selective  $^{13}\text{C}$  pulses used  
94 were Q5 and Q3 (Emsley and Bodenhausen, 1990) of 300  $\mu\text{s}$  and 231  $\mu\text{s}$  for  $90^\circ$  and  $180^\circ$  rotations  
95 respectively; a 900  $\mu\text{s}$  Q3 pulse centered at 53.9 ppm was used for selective inversion of  $\text{C}^\alpha$ . The  $^{15}\text{N}$  pulse  
96 to invert the  $^{15}\text{N}$  proline resonances was a 8000  $\mu\text{s}$  Reburp pulse (Geen and Freeman, 1991); all other  $^{15}\text{N}$   
97 pulses were hard pulses. Decoupling was achieved with waltz65 (100  $\mu\text{s}$ , 2.5 kHz) (Zhou et al., 2007) for  
98  $^1\text{H}$  and with garp4 (250  $\mu\text{s}$ , 1.0 kHz) (Shaka, A. J.; Barker, P. B.; Freeman, 1985) for  $^{15}\text{N}$ . The MOCCA mixing  
99 time (Felli et al., 2009; Furrer et al., 2004) in the (HCA)COCON<sup>Pro</sup> experiment was 350 ms, constituted by  
100 repeated  $(\Delta-180^\circ-\Delta)_{2n}$  units in which  $\Delta=150 \mu\text{s}$  and the  $180^\circ$  pulse was 91.6  $\mu\text{s}$ .

101 The experimental parameters used for the acquisition of the various experiments on  $\alpha$ -synuclein and CBP-  
102 ID4 are reported in Table 1. Spectra were calibrated using DSS as a reference for  $^1\text{H}$  and  $^{13}\text{C}$ ;  $^{15}\text{N}$  was  
103 calibrated indirectly (Markley et al., 1998).



104 **Table 1.** Experimental parameters used.

105

Experiments $\alpha$ -synuclein	Dimension of acquired data			Spectral width (ppm)			NS <sup>a</sup>	d <sub>1</sub> (s) <sup>b</sup>
	t1	t2	t3	F1	F2	F3		
<b><sup>1</sup>H detected</b>								
<sup>1</sup> H- <sup>15</sup> N HSQC	800 ( <sup>15</sup> N)	2048 ( <sup>1</sup> H)		28.1	15.0		2	1.0
<b><sup>13</sup>C detected</b>								
CON	512 ( <sup>15</sup> N)	1024 ( <sup>13</sup> C)		32.0	31.0		2	1.6
CON <sup>Pro</sup>	128 ( <sup>15</sup> N)	1024 ( <sup>13</sup> C)		5.0	31.0		2	1.6
(H)CBCACON <sup>Pro</sup>	128 ( <sup>13</sup> C)	32 ( <sup>15</sup> N)	1024 ( <sup>13</sup> C)	60.0	5.0	30.0	4	1.0
(H)CCCON <sup>Pro</sup>	128 ( <sup>13</sup> C)	32 ( <sup>15</sup> N)	1024 ( <sup>13</sup> C)	70.0	5.0	30.0	4	1.0
(H)CBCANCO <sup>Pro</sup>	128 ( <sup>13</sup> C)	16 ( <sup>15</sup> N)	1024 ( <sup>13</sup> C)	60.0	5.0	30.0	8	1.0
<b><sup>1</sup>H and <sup>13</sup>C detected (using multiple receivers)</b>								
CON/HN	600 ( <sup>15</sup> N)	1024 ( <sup>13</sup> C)		35.0	31.0		2	1.6
	600 ( <sup>15</sup> N)	2048 ( <sup>1</sup> H)		35.0	15.0		4	
<sup>a</sup> number of acquired scans								
<sup>b</sup> inter-scan delay								
Experiments CBP-ID4	Dimension of acquired data			Spectral width (ppm)			NS <sup>a</sup>	d <sub>1</sub> (s) <sup>b</sup>
	t1	t2	t3	F1	F2	F3		
<b><sup>1</sup>H detected</b>								
<sup>1</sup> H- <sup>15</sup> N HSQC	800 ( <sup>15</sup> N)	2048 ( <sup>1</sup> H)		30.0	15.0		2	1.0
<b><sup>13</sup>C detected</b>								
CON	1024 ( <sup>15</sup> N)	1024 ( <sup>13</sup> C)		38.0	30.0		2	2.0
CON <sup>Pro</sup>	170 ( <sup>15</sup> N)	1024 ( <sup>13</sup> C)		6.5	30.0		2	2.0
(H)CBCACON <sup>Pro</sup>	128 ( <sup>13</sup> C)	64 ( <sup>15</sup> N)	1024 ( <sup>13</sup> C)	64.5	6.5	30.0	4	1.0
(H)CCCON <sup>Pro</sup>	128 ( <sup>13</sup> C)	64 ( <sup>15</sup> N)	1024 ( <sup>13</sup> C)	75.7	6.5	30.0	4	1.0
(H)CBCANCO <sup>Pro</sup>	128 ( <sup>13</sup> C)	22 ( <sup>15</sup> N)	1024 ( <sup>13</sup> C)	64.5	6.5	30.0	16	1.0
(HCA)COCON <sup>Pro</sup>	96 ( <sup>13</sup> C)	64 ( <sup>15</sup> N)	1024 ( <sup>13</sup> C)	10.8	6.5	30.0	8	1.5
<sup>a</sup> number of acquired scans								
<sup>b</sup> inter-scan delay								

106

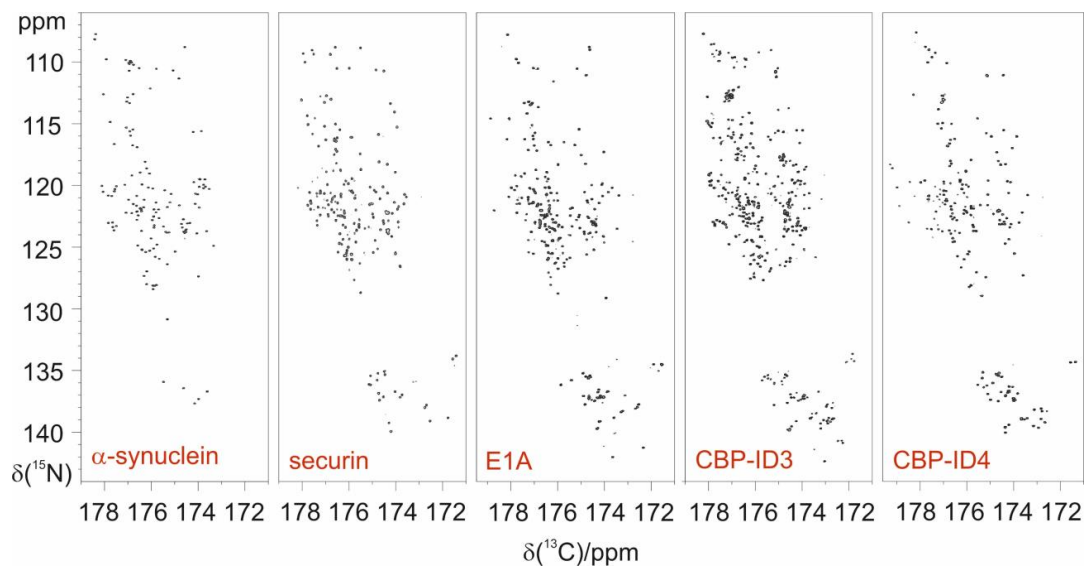


107 **Results and discussion**

108 *Advantages of focusing on proline residues*

109 In highly flexible and disordered proteins contributions to signals' chemical shifts deriving from the local  
110 environment are averaged out leaving mainly those contributions due to the covalent structure of the  
111 polypeptide. Chemical shift ranges predicted for  $^{15}\text{N}$  resonances of imino acids such as proline are quite  
112 different from those predicted for amino acids, as expected from the different chemical structure. The 2D  
113 CON spectra of several disordered proteins of different size and sequence complexity, reported in Figure  
114 1, clearly show that proline residues are quite abundant in IDPs/IDRs and that indeed  $^{15}\text{N}$  resonances of  
115 proline residues fall in a well isolated spectral region.

116



117

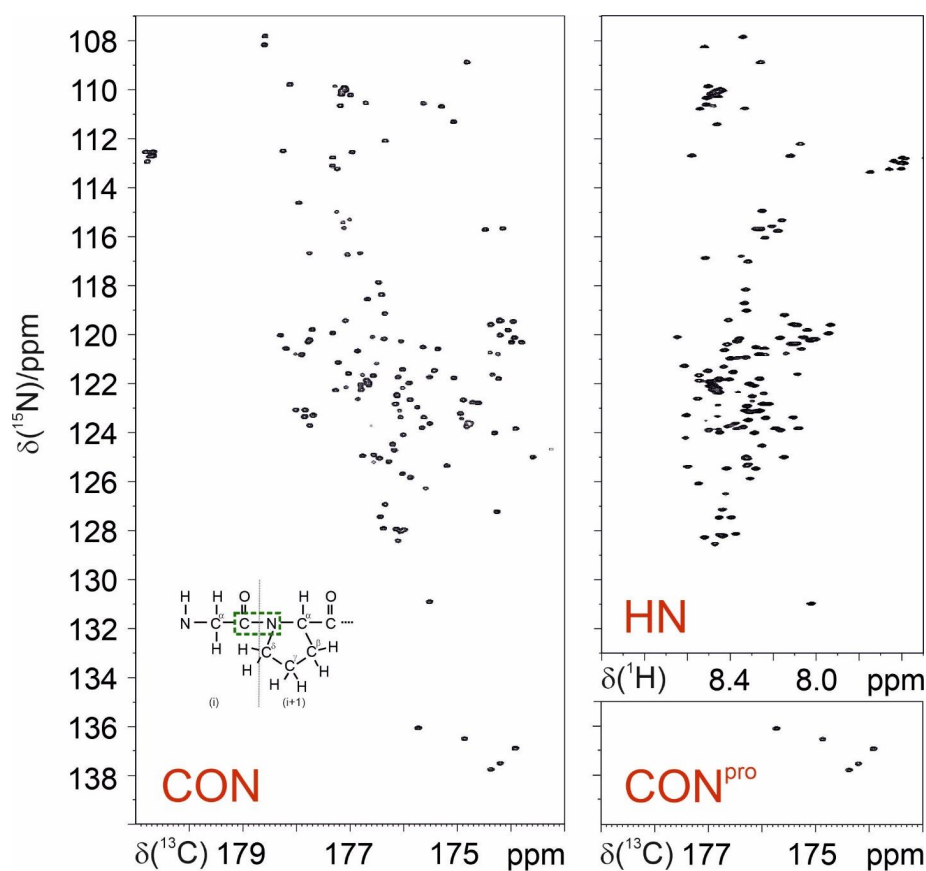
118 **Figure 1.** Proline residues are abundant in IDPs/IDRs and their  $^{15}\text{N}$  resonances can be easily detected. They  
119 fall in a specific, isolated region of the 2D CON spectrum as illustrated by the examples reported in the  
120 figure. From left to right:  $\alpha$ -synuclein (140 aa, 4% Pro)(Bermel et al., 2006b); human securin (200 aa, 11%  
121 Pro)(Bermel et al., 2009); E1A (243 aa, 16% Pro)(Hošek et al., 2016); CBP-ID3 (407 aa 18% Pro)(Contreras-  
122 Martos et al., 2017); CBP-ID4 (207 aa, 22% Pro)(Piai et al., 2016).

123



124 Thus,  $^{15}\text{N}$  resonances of proline residues in IDPs/IDRs can be selectively irradiated enabling us to focus on  
125 this spectral region. This can be achieved through the use of band-selective  $^{15}\text{N}$  pulses as shown for the  
126 simple case of the CON experiment (Murrall et al., 2018): the selective CON spectrum in the proline region  
127 ( $\text{CON}^{\text{pro}}$ , Figure 2) provides the complementary information that is missing in 2D HN correlation  
128 experiments, even when pH and temperature are optimized to enhance the detectability of amide protons  
129 (Figure 2).

130



131

132

133 **Figure 2.** Comparison of the 2D CON (left) and 2D HN (right, top) spectra recorded on  $\alpha$ -synuclein to  
134 illustrate the larger signals' dispersion in the former. The  $\text{CON}^{\text{pro}}$  spectrum (right, bottom), reported below  
135 the HN panel, clearly illustrates how this experiment provides the missing information with respect to that  
136 available in the HN-detected spectrum. In the inset of the 2D CON spectrum a scheme of a  $\text{Gly}_{i-1}\text{-Pro}_i$   
137 dipeptide highlights the nuclei that give rise to the  $\text{C}_{i-1}\text{N}_i$  correlations detected in CON spectra (circled in  
138 green).



139 The same strategy exploiting band-selective  $^{15}\text{N}$  pulses can be used to design experimental variants of  
140 triple resonance  $^{13}\text{C}$  detected experiments to focus on the  $^{15}\text{N}$  proline region and enable us to selectively  
141 detect the desired correlations. When implementing this idea into these experiments, such as the 3D  
142 (H)CBCACON (Bermel et al., 2009),  $^{15}\text{N}$  pulses could all be substituted with band-selective ones. However,  
143 instead of substituting all  $^{15}\text{N}$  pulses, it is sufficient to introduce a  $180^\circ$  band-selective  $^{15}\text{N}$  pulse in one of  
144 the  $\text{C}'_{i-1}\text{-N}_i$  coherence transfer steps to introduce the desired selectivity in the proline region.

145 As an example the pulse sequence of the 3D (H)CBCACON<sup>Pro</sup> experiment is shown in Figure 3. The inclusion  
146 of the  $^{15}\text{N}$  band-selective pulse in the  $\text{C}'\text{-N}$  coherence transfer step is used to generate the  $\text{C}'_{i-1}\text{-N}_i$  antiphase  
147 coherence ( $2\text{C}'_y\text{N}_z$ ) involving the  $^{15}\text{N}$  nuclear spin of proline residues (i); for all other amino acid types the  
148 evolution of the  $\text{C}'_{i-1}\text{-N}_i$  scalar coupling ( $^1J_{\text{C}'_{i-1}\text{N}_i}$ ) is refocused by the  $180^\circ$  band-selective pulse on the  
149 carbonyl carbon nuclei only. To achieve the desired selectivity on the  $^{15}\text{N}$  proline resonances with respect  
150 to those of all other amino acids an 8 ms Reburp pulse (Geen and Freeman, 1991) was used here; this  
151 pulse may appear quite long, but it can be accommodated well in the  $\text{C}'\text{-N}$  coherence transfer block that  
152 requires about 32 ms ( $1/2^1J_{\text{C}'_{i-1}\text{N}_i}$ ). Considering a 8-10 ppm spectral width necessary to cover the  $^{15}\text{N}$   
153 proline-region in the indirect dimension (Figure 1), the implementation of this  $^{15}\text{N}$  band-selective pulse  
154 allows us to reduce the spectral width by a factor of about 4 with respect to that needed to cover the  
155 whole spectral region in which backbone  $^{15}\text{N}$  nuclear spins resonate, that is about 36-40 ppm. This means  
156 that the same resolution can be achieved in a fraction of the time since  $1/4$  (or less) of the FIDs should be  
157 collected, provided sensitivity is not a limiting factor. Thus, it becomes feasible to acquire spectra with  
158 very high resolution, extending the acquisition time in all the indirect dimensions to contrast the reduced  
159 chemical shift dispersion typical of IDPs. Non-uniform sampling strategies (Hoch et al., 2014; Kazimierczuk  
160 et al., 2010, 2011; Robson et al., 2019) can of course be implemented to reduce acquisition times; also in  
161 this case reducing the spectral complexity (the number of cross-peaks is reduced when focusing on proline  
162  $^{15}\text{N}$  resonances only) is expected to contribute to reducing experimental times. Out of the full 3D spectrum  
163 only a small portion, the one containing the information that is completely missing in amide proton  
164 detected experiments, can thus be acquired with the necessary resolution to provide site-specific atomic  
165 information.

166 Since  $\text{C}'$  detected experiments all exploit the  $\text{C}'_{i-1}\text{-N}_i$  correlation, which is an inter-residue correlation  
167 linking the nitrogen of an amino acid (i) to the carbonyl carbon of the previous one (i-1) across the peptide  
168 bond (Figure 2 inset), focusing on proline residues can facilitate the identification of specific  $\text{X}_{i-1}\text{-Pro}_i$  pairs  
169 through inspection of  $\text{C}^\alpha$  and  $\text{C}^\beta$  chemical shifts of the amino acid preceding proline residues. Such



170 information can be achieved through the 3D (H)CBCACON<sup>Pro</sup> experiment and can be very useful to identify  
171 specific pairs such as Gly/Pro, Ala/Pro, Ser/Pro and Thr/Pro. Acquisition of the 3D (H)CCCON<sup>Pro</sup>  
172 experiment, in parallel to the 3D (H)CBCACON<sup>Pro</sup>, provides information on aliphatic <sup>13</sup>C nuclear chemical  
173 shifts of the whole side chain. This contributes to narrowing down the possibilities in all cases in which it  
174 is not possible to identify the type of amino acid preceding the proline only considering their <sup>13</sup>C<sup>α</sup> and <sup>13</sup>C<sup>β</sup>  
175 chemical shifts. This is the case for example of Arg/Lys/Gln or Phe/Leu.

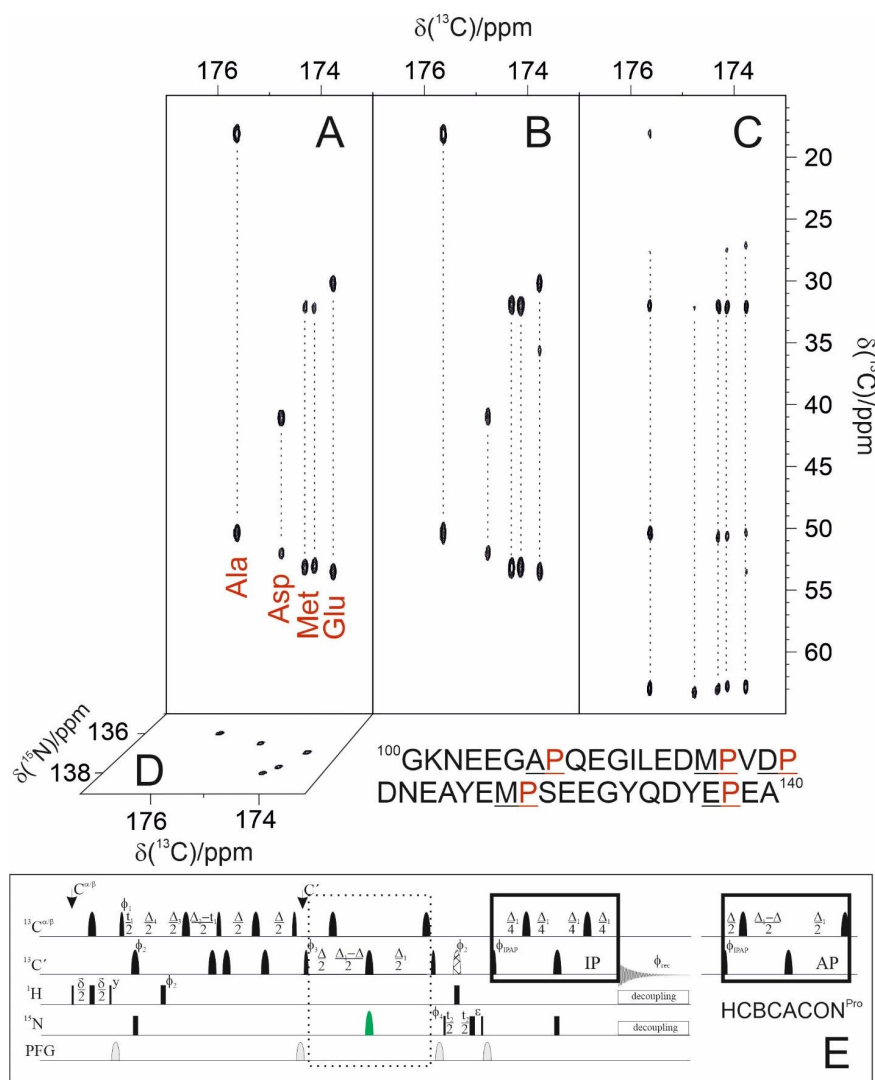
176 Similarly, the insertion of the <sup>15</sup>N band-selective pulse in the proline region in the 3D (H)CBCANCO (Bermel  
177 et al., 2006a) enables us to detect the <sup>13</sup>C resonances of the whole proline ring, providing the  
178 complementary information for sequence-specific assignment. The closed proline ring introduces an  
179 additional heteronuclear scalar coupling (<sup>1</sup>J<sub>Ni-Cδi</sub>) that also provides the correlations with <sup>13</sup>C<sup>δ</sup> and <sup>13</sup>C<sup>γ</sup>, in  
180 parallel to <sup>13</sup>C<sup>α</sup> and <sup>13</sup>C<sup>β</sup> chemical shifts. Indeed the band-selective pulses used for the <sup>13</sup>C aliphatic region  
181 cover also <sup>13</sup>C<sup>γ</sup> and <sup>13</sup>C<sup>δ</sup> resonances (not only <sup>13</sup>C<sup>α</sup> and <sup>13</sup>C<sup>β</sup> ones). In addition analysis of the observed  
182 chemical shifts for proline side chains can be correlated to the local conformation, in particular to the  
183 cis/trans isomers of the peptide bond involving proline nitrogen nuclei (Schubert et al., 2002; Shen and  
184 Bax, 2010). Finally, additional information for sequence-specific assignment can be achieved by exploiting  
185 the same approach for the COCON experiment in its <sup>13</sup>C-start (Bermel et al., 2006b; Felli et al., 2009) as  
186 well and in its <sup>1</sup>H-start variants (Mateos et al., 2020).

187

#### 188 *Assignment strategy*

189 To illustrate the approach, experiments were acquired on the well-known IDP α-synuclein. Even if this  
190 protein only contains a little number of proline residues (5/140), they are all clustered in a small portion  
191 of it (108-138) and thus constitute about 15% of the amino acids in this region. Furthermore, this terminus  
192 has a very peculiar amino acidic composition (36% Asp/Glu, 9% Tyr) and it was shown to be the part of  
193 the protein that is involved in sensing calcium concentration jumps associated with the transmission of  
194 nerve signals (Binolfi et al., 2006; Lautenschläger et al., 2018; Nielsen et al., 2001). Proline residues,  
195 embedded in two motifs (DPD and EPE), were shown to facilitate the interaction of carboxylate side chains  
196 of Asp and Glu with calcium, even in a flexible, disordered state (Pontoriero et al., 2020).

197 Focusing on the proline <sup>15</sup>N region in case of α-synuclein greatly simplifies the spectral complexity enabling  
198 us to illustrate the sequence-specific assignment of the resonances just by visual inspection of the first  
199 planes of the 3D spectra described here (Figure 3).



200

201 **Figure 3.** The implementation of the proposed strategy on  $\alpha$ -synuclein renders NMR spectra so  
 202 informative that proline resonances can be assigned just by visual inspection of the figure. To this end the  
 203 first  $^{13}\text{C}$ - $^{13}\text{C}$  planes of the 3D (H)CBCACON<sup>Pro</sup> (A), 3D (H)CCCON<sup>Pro</sup> (B), 3D (H)CBCANCO<sup>Pro</sup> (C) are shown; the  
 204  $^{13}\text{C}$ - $^{15}\text{N}$  plane of the 3D (H)CBCACON<sup>Pro</sup> is also shown (D). The portion of the primary sequence of  $\alpha$ -  
 205 synuclein hosting its five proline residues is also reported (bottom right). The pulse sequence to acquire  
 206 the 3D (H)CBCACON<sup>Pro</sup> experiment (E) is reported as an example of the implementation of the proposed  
 207 approach (dotted box). The delays are:  $\epsilon = t_2(0)$ ,  $\delta = 3.6$  ms,  $\Delta = 9$  ms,  $\Delta_1 = 25$  ms,  $\Delta_2 = 8$  ms,  $\Delta_3 = \Delta_2 - \Delta_4 =$   
 208  $5.8$  ms,  $\Delta_4 = 2.2$  ms. The phase cycle is:  $\phi_1 = x, -x$ ;  $\phi_2 = 8(x), 8(-x)$ ;  $\phi_3 = 4(x), 4(-x)$ ;  $\phi_4 = 2(x), 2(-x)$ ;  $\phi_{\text{IPAP}}(\text{IP}) =$   
 209  $x$ ;  $\phi_{\text{IPAP}}(\text{AP}) = -y$ ;  $\phi_{\text{rec}} = x, -x, -x, x, -x, x, x, -x$ . Quadrature detection was obtained by incrementing phase  $\phi_3$   
 210 ( $t_1$ ) and  $\phi_4$  ( $t_2$ ) in a States-TPPI manner.

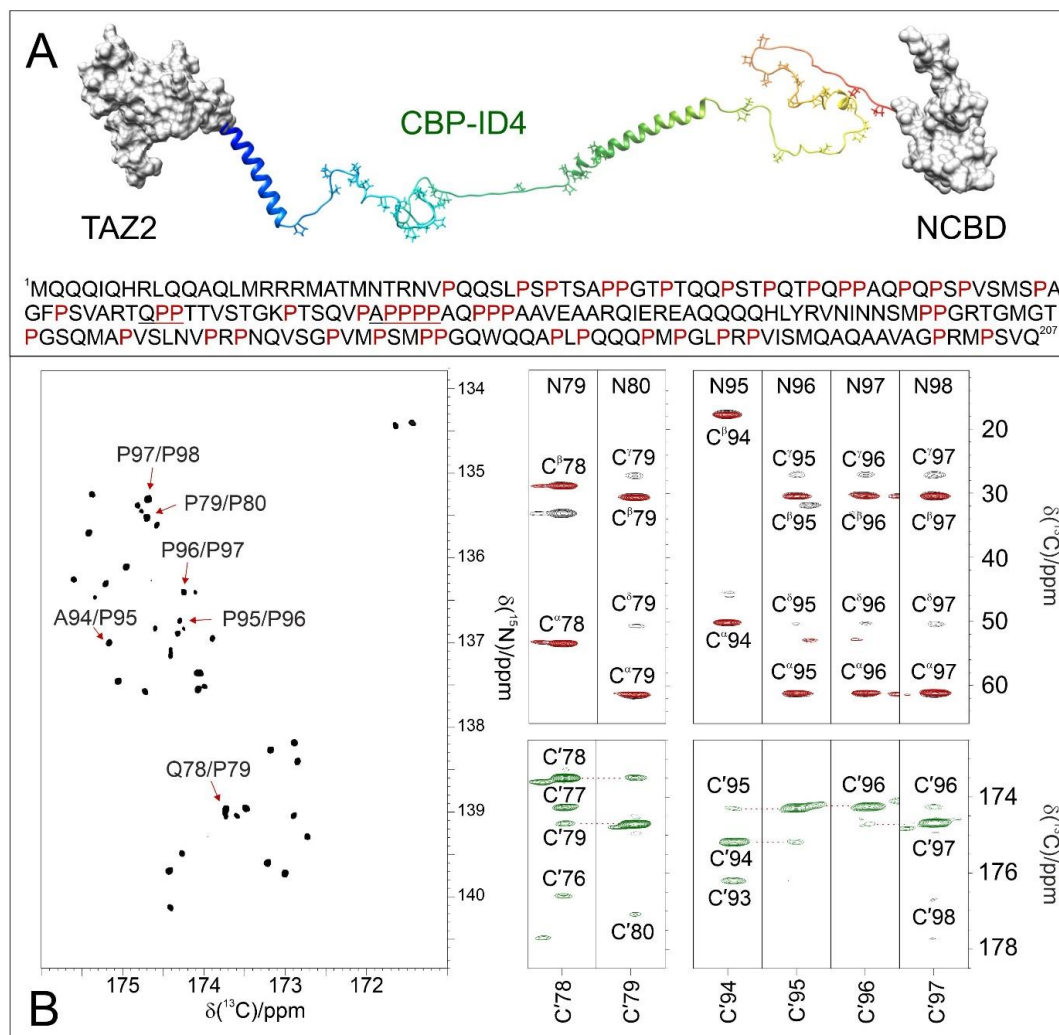


211 Indeed, the C'-N projections of the 3D spectra ( $^{13}\text{C}$ - $^{15}\text{N}$  planes) show that the cross-peaks are well resolved  
212 in both dimensions; selection of the  $^{15}\text{N}$  proline region enables us to differentiate the signals through the  
213 carbonyl carbon chemical shifts of the preceding amino acid. Therefore inspection of the first  $^{13}\text{C}$ - $^{13}\text{C}$  plane  
214 of the 3D (H)CBCACON<sup>Pro</sup> experiment (Figure 3A) shows the distinctive  $^{13}\text{C}^{\alpha}$  and  $^{13}\text{C}^{\beta}$  chemical shift patterns  
215 of the residues preceding proline that, by comparison with the primary sequence of the protein, already  
216 suggest us the identity of three residue pairs: Ala-Pro, Asp-Pro, Glu-Pro. These can thus be assigned to Ala  
217 107-Pro 108, Asp 119-Pro 120, Glu 138-Pro 139. Comparison with the first  $^{13}\text{C}$ - $^{13}\text{C}$  plane of the 3D  
218 (H)CCCON<sup>Pro</sup> (Figure 3B) confirms that an extra cross peak can be detected for the Glu-Pro pair, as  
219 expected for amino acids which have a side chain with more than two aliphatic carbon atoms. The  
220 remaining signals derive from the two Met-Pro pairs, in agreement with the observed chemical shifts.  
221 They can be assigned in a sequence specific manner by comparison of these spectra with the  
222 complementary ones based on amide proton detection. The final panel shows the first  $^{13}\text{C}$ - $^{13}\text{C}$  plane of  
223 the 3D (H)CBCANCO<sup>Pro</sup> (Figure 3C). This experiment reveals the correlations of the  $^{15}\text{N}$  with  $^{13}\text{C}^{\alpha}$  and  $^{13}\text{C}^{\beta}$   
224 within each amino acid. In the case of proline, the closed ring introduces additional scalar couplings that  
225 are responsible for two additional cross-peaks, the ones of the  $^{15}\text{N}$  with  $^{13}\text{C}^{\gamma}$  and  $^{13}\text{C}^{\delta}$ , as clearly observed  
226 in Figure 3. Chemical shifts show only minor differences between the resonances but still significant to  
227 discriminate the different residues provided spectra are acquired with high resolution.

228

#### 229 *A challenging case*

230 A compelling example of complexity is provided by the ID4 flexible linker of CREB-binding protein (CBP), a  
231 large transcription co-regulator (Dyson and Wright, 2016). CBP-ID4 connects two well-characterized  
232 globular domains (TAZ2, 92 amino acids and NCB2, 59 amino acids)(De Guzman et al., 2000; Kjaergaard  
233 et al., 2010) and is constituted by 207 amino acids out of which 45 are proline residues, including several  
234 repeated PP motives (Piai et al., 2016) (Figure 4A). The 2D CON<sup>Pro</sup> spectrum of CBP-ID4, reported in Figure  
235 4B (left panel), shows the  $\text{C}'_{i-1}$ - $\text{N}_i$  correlations of proline residues of ID4. Interestingly, despite the small  
236 spectral region, a high number of resolved resonances is observed. The initial count of cross-peaks in this  
237 spectrum reveals 42 out of the 45 expected correlations, highlighting the potential of this experimental  
238 strategy for the investigation of IDRs/IDPs of increasing complexity. The excellent chemical shift dispersion  
239 of the inter-residue  $\text{C}'_{i-1}$ - $\text{N}_i$  correlations is certainly one of the most important aspects to reduce cross peak  
240 overlap. Resolution is further enhanced in this region by the narrow linewidths of proline  $^{15}\text{N}$  resonances  
241 due to the lack of the dipolar contribution of an amide proton to the transverse relaxation.



242

243

244 **Figure 4.** The case of CBP-ID4 (residues 1851–2057 of human CBP). (A) One of the possible conformations  
 245 of the CBP-ID4 fragment (blue-to-red ribbons) and the two flanking domains TAZ2 and NCBD clearly  
 246 demonstrate that in this region of CBP the intrinsically disordered part is highly prevalent with respect to  
 247 ordered ones. The amino acid sequence of CBP-ID4 is also reported. (B) The 2D CON<sup>Pro</sup> spectrum shown  
 248 on the left, which at first sight could seem like a 2D spectrum of a small globular protein, reports the  
 249 proline fingerprint of this complex IDR. Several strips extracted from the 3D (H)CBCACON<sup>Pro</sup> (black  
 250 contours), 3D (H)CCCON<sup>Pro</sup> (red contours), 3D (HCA)COCON<sup>Pro</sup> (green contours) are shown to illustrate the  
 251 information available for sequence specific resonance assignment of this proline-rich fragment of CBP-  
 252 ID4.



253 These two features contribute to establishing this spectral region as a key one for the assignment of a  
254 large IDR. Indeed, when passing from 2D to 3D experiments, long acquisition times in the  $^{15}\text{N}$  dimension  
255 are possible and enable us to provide the extra contribution to resolution enhancement needed to focus  
256 on complex IDRs and to collect additional information on the proline residues and their neighbouring  
257 amino acids. As an example of the quality of the spectra, Figure 4B reports several strips extracted from  
258 the pro-selective 3D experiments that were essential for the investigation of a particularly proline-rich  
259 region of ID4, the one in between two partially populated  $\alpha$ -helices (Piai et al., 2016). This is composed by  
260 27 prolines (out of 76 amino acids) which constitute 35% of the amino acids in this region including several  
261 proline-rich motifs (PXP, PXXP, PP as well as PPP and PPPP). The strips extracted from the 3D  
262 (H)CBCACON<sup>Pro</sup> and 3D (H)CCCON<sup>Pro</sup> (Figure 4B, right panels, black and red contours respectively) are very  
263 useful to identify the  $X_{i-1}$ -Pro<sub>*i*</sub> pairs that match in this case with a Gln-Pro and an Ala-Pro pair as well as  
264 several Pro-Pro ones. The 3D (H)CBCANCO<sup>Pro</sup> completes the picture providing information about  $^{13}\text{C}$   
265 resonances of each proline ring ( $\text{C}^\alpha$ ,  $\text{C}^\beta$ ,  $\text{C}^\gamma$ ,  $\text{C}^\delta$ , not shown for sake of clarity of the figure). However in  
266 regions with a high abundance of proline residues additional information is needed for their sequence-  
267 specific assignment. To this end the 3D (HCA)COCON<sup>Pro</sup> (Figure 4B, right panels, green contours) is very  
268 useful, as demonstrated for these two proline-rich fragments. This experiment, which includes an  
269 isotropic mixing element in the carbonyl region (MOCCA in this case (Felli et al., 2009; Furrer et al., 2004)),  
270 enables us to detect correlations of a carbonyl with the neighbouring ones through the small  $^3J_{\text{CC}}$  scalar  
271 couplings. In case of proline residues the most intense cross-peak is generally observed for the preceding  
272 amino acid ( $\text{C}'_{i-2}$ ). However additional peaks are detected also with neighbouring ones and support the  
273 sequence-specific assignment process.

274 It is interesting to note, once the sequence-specific assignment becomes available, that  $\text{C}'_{i-1}$ - $\text{N}_i$  correlations  
275 fall in distinctive spectral regions of the CON<sup>Pro</sup> 2D spectrum, as already pointed out for selected residue  
276 pairs such as Gly-Pro, Ser-Pro, Thr-Pro, Val-Pro (Murrall et al., 2018). For example, inspection of Figure 1  
277 allows us to identify Gly-Pro pairs in all the CON spectra of different proteins from their characteristic  
278 chemical shifts (in the top-right portion of the proline region). An additional contribution towards smaller  
279  $^{15}\text{N}$  chemical shifts can also be identified in cases in which more than one proline follows a specific amino  
280 acid-type such as for Ala-Pro, Met-Pro and Gln-Pro cross peaks that are shifted to lower  $^{15}\text{N}$  chemical shifts  
281 when an additional proline follows in the primary sequence. These effects are likely to originate from a  
282 combination of effects deriving from the covalent structure (primary sequence in this case) as well as from  
283 local conformations. Needless to say that the experimental investigation of these aspects in more detail  
284 constitutes an important point to describe the structural and dynamic properties at atomic resolution of



285 the proline-rich parts of highly flexible IDRs. The proposed experiments are thus expected to become of  
286 general applicability for studies of IDPs/IDRs in solution.

287 The data generated on proline-rich sequences are of course very relevant to populate the BMRB with  
288 more information on proline residues in highly flexible protein regions. This in turn will generate more  
289 accurate reference data in chemical shift databases to determine local structural propensities through the  
290 comparison of experimental shifts with reference ones (Camilloni et al., 2012; Tamiola et al., 2010)  
291 improving our understanding of the importance of transient secondary structure elements in determining  
292 protein function. On this respect, CBP itself provides another enlightening example with CBP-ID3 (residues  
293 674-1079 of CBP), which features a high number of proline residues (75 out of 406 residues) representing  
294 18% of its primary sequence. The distribution in this case is along the entire sequence but less frequent  
295 toward the end, where a  $\beta$ -strand conformation propensity is sampled. Also in this case the distribution  
296 of proline residues is important in shaping the conformational space accessible to the polypeptide,  
297 facilitating the interaction with protein's partners (Contreras-Martos et al., 2017).

298 Determination of additional observables, such as the  $^3J_{CC}$  through the 3D (HCA)COCON<sup>Pro</sup> experiment or  
299 of different ones through modified experimental variants of these experiments are expected to contribute  
300 to the characterization of novel motives in IDRs/IDPs.

301 The experimental strategy proposed here focuses on a remarkably small spectral region which however  
302 turns out to be one of the most interesting ones, in particular in the perspective of studying IDPs/IDRs of  
303 increasing complexity, somehow reminiscent of other strategies that have been proposed in which only  
304 selected residue types are investigated to access information on challenging systems (such as for example  
305 the studies of large systems enabled by Methyl-TROSY spectroscopy (Kay, 2011; Schütz and Sprangers,  
306 2020). Interestingly the analysis of the NMR spectra presented here enables one to classify the observed  
307 cross peaks into residue types, also in absence of sequence-specific assignment. This might provide  
308 interesting information for complex IDPs/IDRs in which one is interested in the investigation of the  
309 contribution of specific residue types, such as to monitor the occurrence of post-translational  
310 modifications or even other phenomena that are more difficult to investigate like liquid-liquid phase  
311 separation.



312 **Conclusions and perspectives**

313 Detection and assignment of proline-rich regions of highly flexible intrinsically disordered proteins allows  
314 us to have a glimpse on the ways in which proline residues encode specific properties in IDRs/IDPs by  
315 simply tuning their distribution along the primary sequence. NMR spectroscopy is particularly well suited  
316 for the task, since proline residues have attractive features from the NMR point of view, starting from the  
317 peculiar chemical shifts of  $^{15}\text{N}$  nuclear spins. In addition, the lack of the attached amide proton implies  
318 that one of the major contributions to relaxation of  $^{15}\text{N}$  spins is absent and thus proline nitrogen signals  
319 have small linewidths. These characteristics make them a very useful starting point for sequential  
320 assignment purposes and structure characterization. Furthermore, they provide a set of NMR signals with  
321 promising properties to enable high-resolution studies of increasingly large IDPs/IDRs.

322 Several approaches either based on  $\text{H}^{\text{N}}$  or on  $\text{H}^{\alpha}$  direct detection have been proposed to bypass the  
323 problem introduced in sequence-specific assignment by the lack of amide protons typical of proline  
324 residues (Hellman et al., 2014; Kanelis et al., 2000; Karjalainen et al., 2020; Löhr et al., 2000; Mäntylahti  
325 et al., 2010; Tossavainen et al., 2020; Wong et al., 2018). While these can result useful for systems with  
326 moderate complexity ( $\text{H}^{\alpha}$  detection) or for systems that feature isolated proline residues in the primary  
327 sequence ( $\text{H}^{\text{N}}/\text{H}^{\alpha}$ ), they are not as efficient for complex IDRs/IDPs in which high resolution is mandatory  
328 and in which often consecutive proline residues are encountered. Thus, the proposed experiments are  
329 crucial to assign intrinsically disordered protein regions presenting many repeated motives including  
330 proline residues as well as poly-proline segments.

331 Since NMR probeheads with high  $^{13}\text{C}$  sensitivity have become widely available, it is expected that this set  
332 of experiments will be applied as an easy-to-use tool also to complement  $\text{H}^{\text{N}}$ -based assignment.

333

334 **Acknowledgments**

335 The support of the CERM/CIRMMP center of Instruct-ERIC is gratefully acknowledged. This work has been  
336 funded in part by a grant of the Fondazione CR Firenze and by the Italian Ministry of University and  
337 Research (FOE funding). Maria Grazia Murralli, Letizia Pontoriero and Marco Schiavina are acknowledged  
338 for their contribution in the early stages of the project.

339

340



## 341 References

- 342 Bermel, W., Bertini, I., Felli, I. C., Kümmerle, R. and Pierattelli, R.: Novel  $^{13}\text{C}$  direct detection experiments,  
343 including extension to the third dimension, to perform the complete assignment of proteins, *J. Magn.*  
344 *Reson.*, 178(1), 56–64, doi:10.1016/j.jmr.2005.08.011, 2006a.
- 345 Bermel, W., Bertini, I., Felli, I. C., Lee, Y.-M., Luchinat, C. and Pierattelli, R.: Protonless NMR experiments  
346 for sequence-specific assignment of backbone nuclei in unfolded proteins, *J. Am. Chem. Soc.*, 128(12),  
347 3918–3919, doi:10.1021/ja0582206, 2006b.
- 348 Bermel, W., Bertini, I., Csizmok, V., Felli, I. C., Pierattelli, R. and Tompa, P.: H-start for exclusively  
349 heteronuclear NMR spectroscopy: the case of intrinsically disordered proteins, *J. Magn. Reson.*, 198(2),  
350 275–281, doi:10.1016/j.jmr.2009.02.012, 2009.
- 351 Binolfi, A., Rasia, R. M., Bertoncini, C. W., Ceolin, M., Zweckstetter, M., Griesinger, C., Jovin, T. M. and  
352 Fernández, C. O.: Interaction of  $\alpha$ -synuclein with divalent metal ions reveals key differences: a link  
353 between structure, binding specificity and fibrillation enhancement, *J. Am. Chem. Soc.*, 128(30), 9893–  
354 9901, doi:10.1021/ja0618649, 2006.
- 355 Camilloni, C., De Simone, A., Vranken, W. F. and Vendruscolo, M.: Determination of secondary structure  
356 populations in disordered states of proteins using nuclear magnetic resonance chemical shifts,  
357 *Biochemistry*, 51(11), 2224–2231, doi:10.1021/bi3001825, 2012.
- 358 Chaves-Arquero, B., Pantoja-Uceda, D., Roque, A., Ponte, I., Suau, P. and Jiménez, M. A.: A CON-based  
359 NMR assignment strategy for pro-rich intrinsically disordered proteins with low signal dispersion: the C-  
360 terminal domain of histone H1.0 as a case study, *J. Biomol. NMR*, 72(3–4), 139–148,  
361 doi:10.1007/s10858-018-0213-2, 2018.
- 362 Contreras-Martos, S., Piai, A., Kosol, S., Varadi, M., Bekesi, A., Lebrun, P., Volkov, A. N., Gevaert, K.,  
363 Pierattelli, R., Felli, I. C. and Tompa, P.: Linking functions: an additional role for an intrinsically disordered  
364 linker domain in the transcriptional coactivator CBP, *Sci. Rep.*, 7(1), 4676, doi:10.1038/s41598-017-  
365 04611-x, 2017.
- 366 Dunker, A. K., Oldfield, C. J., Meng, J., Romero, P., Yang, J. Y., Chen, J. W., Vacic, V., Obradovic, Z. and  
367 Uversky, V. N.: The unfoldomics decade: an update on intrinsically disordered proteins, *BMC Genomics*,  
368 9(SUPPL. 2), 1–26, doi:10.1186/1471-2164-9-S2-S1, 2008.
- 369 Dyson, H. Jane; Wright, P.: Nuclear magnetic resonance methods for elucidation of structure and  
370 dynamics in disordered states, *Methods Enzymol.*, 339, 258–270, 2001.
- 371 Dyson, H. J. and Wright, P. E.: Role of intrinsic protein disorder in the function and interactions of the  
372 transcriptional coactivators CREB-binding Protein (CBP) and p300, *J. Biol. Chem.*, 291(13), 6714–6722,  
373 doi:10.1074/jbc.R115.692020, 2016.
- 374 Emsley, L. and Bodenhausen, G.: Gaussian pulse cascades: new analytical functions for rectangular  
375 selective inversion and in-phase excitation in NMR, *Chem. Phys. Lett.*, 165(6), 469–476,  
376 doi:10.1016/0009-2614(90)87025-M, 1990.
- 377 Felli, I. C. and Pierattelli, R.: Novel methods based on  $^{13}\text{C}$  detection to study intrinsically disordered  
378 proteins, *J. Magn. Reson.*, 241(1), 115–125, doi:10.1016/j.jmr.2013.10.020, 2014.
- 379 Felli, I. C., Pierattelli, R., Glaser, S. J. and Luy, B.: Relaxation-optimised Hartmann-Hahn transfer using a  
380 specifically tailored MOCCA-XY16 mixing sequence for carbonyl-carbonyl correlation spectroscopy in  $^{13}\text{C}$



- 381 direct detection NMR experiments, *J. Biomol. NMR*, 43(3), doi:10.1007/s10858-009-9302-6, 2009.
- 382 Furrer, J., Kramer, F., Marino, J. P., Glaser, S. J. and Luy, B.: Homonuclear Hartmann-Hahn transfer with  
383 reduced relaxation losses by use of the MOCCA-XY16 multiple pulse sequence, *J. Magn. Reson.*, 166(1),  
384 39–46, doi:10.1016/j.jmr.2003.09.013, 2004.
- 385 Geen, H. and Freeman, R.: Band-selective radiofrequency pulses, *J. Magn. Reson.*, 93(1), 93–141,  
386 doi:10.1016/0022-2364(91)90034-Q, 1991.
- 387 Gibbs, E. B., Lu, F., Portz, B., Fisher, M. J., Medellin, B. P., Laremore, T. N., Zhang, Y. J., Gilmour, D. S. and  
388 Showalter, S. A.: Phosphorylation induces sequence-specific conformational switches in the RNA  
389 polymerase II C-terminal domain, *Nat. Commun.*, 8(May), 1–11, doi:10.1038/ncomms15233, 2017.
- 390 Gil, S., Hošek, T., Solyom, Z., Kümmerle, R., Brutscher, B., Pierattelli, R. and Felli, I. C.: NMR spectroscopic  
391 studies of intrinsically disordered proteins at near-physiological conditions, *Angew. Chemie - Int. Ed.*,  
392 52(45), 11808–11812, doi:10.1002/anie.201304272, 2013.
- 393 De Guzman, R. N., Liu, H. Y., Martinez-Yamout, M., Dyson, H. J. and Wright, P. E.: Solution structure of  
394 the TAZ2 (CH3) domain of the transcriptional adaptor protein CBP, *J. Mol. Biol.*, 303(2), 243–253,  
395 doi:10.1006/jmbi.2000.4141, 2000.
- 396 Haba, N. Y., Gross, R., Novacek, J., Shaked, H., Zidek, L., Barda-Saad, M. and Chill, J. H.: NMR determines  
397 transient structure and dynamics in the disordered C-terminal domain of WASp interacting protein,  
398 *Biophys. J.*, 105(2), 481–493, doi:10.1016/j.bpj.2013.05.046, 2013.
- 399 Hellman, M., Piirainen, H., Jaakola, V. P. and Permi, P.: Bridge over troubled proline: Assignment of  
400 intrinsically disordered proteins using (HCA)CON(CAN)H and (HCA)N(CA)CO(N)H experiments  
401 concomitantly with HNCO and i(HCA)CO(CA)NH, *J. Biomol. NMR*, 58(1), 49–60, doi:10.1007/s10858-013-  
402 9804-0, 2014.
- 403 Hoch, J. C., Maciejewski, M. W., Mobli, M., Schuyler, A. D. and Stern, A. S.: Nonuniform sampling and  
404 maximum entropy reconstruction in multidimensional NMR, *Acc. Chem. Res.*, 47(2), 708–717,  
405 doi:10.1021/ar400244v, 2014.
- 406 Hošek, T., Calçada, E. O., Nogueira, M. O., Salvi, M., Pagani, T. D., Felli, I. C. and Pierattelli, R.: Structural  
407 and dynamic characterization of the molecular hub early region 1A (E1A) from human adenovirus,  
408 *Chem. - A Eur. J.*, 22(37), doi:10.1002/chem.201602510, 2016.
- 409 Hsu, S.-T. D., Bertoncini, C. W. and Dobson, C. M.: Use of protonless NMR spectroscopy to alleviate the  
410 loss of information resulting from exchange-broadening, *J. Am. Chem. Soc.*, 131(21), 7222–7223,  
411 doi:10.1021/ja902307q, 2009.
- 412 Huang, C., Ren, G., Zhou, H. and Wang, C.: A new method for purification of recombinant human  $\alpha$ -  
413 synuclein in *Escherichia coli*, *Protein Expr. Purif.*, 42(1), 173–177, doi:10.1016/j.pep.2005.02.014, 2005.
- 414 Kanelis, V., Donaldson, L., Muhandiram, D. R., Rotin, D., Forman-Kay, J. D. and Kay, L. E.: Sequential  
415 assignment of proline-rich regions in proteins: Application to modular binding domain complexes, *J.*  
416 *Biomol. NMR*, 16(3), 253–259, doi:10.1023/A:1008355012528, 2000.
- 417 Karjalainen, M., Tossavainen, H., Hellman, M. and Permi, P.: HACANCOi: a new H $\alpha$ -detected experiment  
418 for backbone resonance assignment of intrinsically disordered proteins, *J. Biomol. NMR*, 74(12), 741–  
419 752, doi:10.1007/s10858-020-00347-5, 2020.



- 420 Kay, L. E.: Solution NMR spectroscopy of supra-molecular systems, why bother? A methyl-TROSY view, *J.*  
421 *Magn. Reson.*, 210(2), 159–170, doi:10.1016/j.jmr.2011.03.008, 2011.
- 422 Kazimierczuk, K., Stanek, J., Zawadzka-Kazimierczuk, A. and Koźmiński, W.: Random sampling in  
423 multidimensional NMR spectroscopy, *Prog. Nucl. Magn. Reson. Spectrosc.*, 57(4), 420–434,  
424 doi:10.1016/j.pnmrs.2010.07.002, 2010.
- 425 Kazimierczuk, K., Misiak, M., Stanek, J., Zawadzka-Kazimierczuk, A. and Koźmiński, W.: Generalized  
426 Fourier transform for non-uniform sampled data, in *Topics in current chemistry*, vol. 312, pp. 79–124.,  
427 2011.
- 428 Kjaergaard, M., Teilum, K. and Poulsen, F. M.: Conformational selection in the molten globule state of  
429 the nuclear coactivator binding domain of CBP, *Proc. Natl. Acad. Sci. U. S. A.*, 107(28), 12535–12540,  
430 doi:10.1073/pnas.1001693107, 2010.
- 431 Knoblich, K., Whittaker, S., Ludwig, C., Michiels, P., Jiang, T., Schaffhausen, B. and Günther, U.: Backbone  
432 assignment of the N-terminal polyomavirus large T antigen, *Biomol. NMR Assign.*, 3(1), 119–123,  
433 doi:10.1007/s12104-009-9155-7, 2009.
- 434 Kurzbach, D., Canet, E., Flamm, A. G., Jhajharia, A., Weber, E. M. M., Konrat, R. and Bodenhausen, G.:  
435 Investigation of intrinsically disordered proteins through exchange with hyperpolarized water, *Angew.*  
436 *Chemie - Int. Ed.*, 56(1), 389–392, doi:10.1002/anie.201608903, 2017.
- 437 Lautenschläger, J., Stephens, A. D., Fusco, G., Ströhl, F., Curry, N., Zacharopoulou, M., Michel, C. H.,  
438 Laine, R., Nespovitaya, N., Fantham, M., Pinotsi, D., Zago, W., Fraser, P., Tandon, A., St George-Hyslop,  
439 P., Rees, E., Phillips, J. J., De Simone, A., Kaminski, C. F. and Schierle, G. S. K.: C-terminal calcium binding  
440 of  $\alpha$ -synuclein modulates synaptic vesicle interaction, *Nat. Commun.*, 9(1), doi:10.1038/s41467-018-  
441 03111-4, 2018.
- 442 Van Der Lee, R., Buljan, M., Lang, B., Weatheritt, R. J., Daughdrill, G. W., Dunker, A. K., Fuxreiter, M.,  
443 Gough, J., Gsponer, J., Jones, D. T., Kim, P. M., Kriwacki, R. W., Oldfield, C. J., Pappu, R. V., Tompa, P.,  
444 Uversky, V. N., Wright, P. E. and Babu, M. M.: Classification of intrinsically disordered regions and  
445 proteins, *Chem. Rev.*, 114(13), 6589–6631, doi:10.1021/cr400525m, 2014.
- 446 Löhr, F., Pfeiffer, S., Lin, Y. J., Hartleib, J., Klimmek, O. and Rüterjans, H.: HNCAN pulse sequences for  
447 sequential backbone resonance assignment across proline residues in perdeuterated proteins, *J. Biomol.*  
448 *NMR*, 18(4), 337–346, doi:10.1023/A:1026737732576, 2000.
- 449 Lopez, J., Schneider, R., Cantrelle, F. X., Huvent, I. and Lippens, G.: Studying intrinsically disordered  
450 proteins under true in vivo conditions by combined cross-polarization and carbonyl-detection NMR  
451 spectroscopy, *Angew. Chemie - Int. Ed.*, 55(26), 7418–7422, doi:10.1002/anie.201601850, 2016.
- 452 Lu, K. P., Finn, G., Lee, T. H. and Nicholson, L. K.: Prolyl cis-trans isomerization as a molecular timer, *Nat.*  
453 *Chem. Biol.*, 3(10), 619–629, doi:10.1038/nchembio.2007.35, 2007.
- 454 MacArthur, M. W. and Thornton, J. M.: Influence of proline residues on protein conformation, *J. Mol.*  
455 *Biol.*, 218(2), 397–412, doi:10.1016/0022-2836(91)90721-H, 1991.
- 456 Mäntylähti, S., Aitio, O., Hellman, M. and Permi, P.: HA-detected experiments for the backbone  
457 assignment of intrinsically disordered proteins, *J. Biomol. NMR*, 47(3), 171–181, doi:10.1007/s10858-  
458 010-9421-0, 2010.
- 459 Markley, J. L., Bax, A., Arata, Y., Hilbers, C. W., Kaptein, R., Sykes, B. D., Wright, P. E. and Wüthrich, K.:



- 460 Recommendations for the presentation of NMR structures of proteins and nucleic acids, *J. Biomol. NMR*,  
461 12(1), 1–23, doi:10.1023/A:1008290618449, 1998.
- 462 Mateos, B., Conrad-Billroth, C., Schiavina, M., Beier, A., Kontaxis, G., Konrat, R., Felli, I. C. and Pierattelli,  
463 R.: The ambivalent role of proline residues in an intrinsically disordered protein: from disorder  
464 promoters to compaction facilitators, *J. Mol. Biol.*, 432(9), doi:10.1016/j.jmb.2019.11.015, 2020.
- 465 Murralli, M. G., Piai, A., Bermel, W., Felli, I. C. and Pierattelli, R.: Proline fingerprint in intrinsically  
466 disordered proteins, *ChemBioChem*, 19(15), 1625–1629, doi:10.1002/cbic.201800172, 2018.
- 467 Nielsen, M. S., Vorum, H., Lindersson, E. and Jensen, P. H.: Ca<sup>2+</sup> Binding to  $\alpha$ -synuclein regulates ligand  
468 binding and oligomerization, *J. Biol. Chem.*, 276(25), 22680–22684, doi:10.1074/jbc.M101181200, 2001.
- 469 Olsen, G. L., Szekeley, O., Mateos, B., Kadeřávek, P., Ferrage, F., Konrat, R., Pierattelli, R., Felli, I. C.,  
470 Bodenhausen, G., Kurzbach, D. and Frydman, L.: Sensitivity-enhanced three-dimensional and carbon-  
471 detected two-dimensional NMR of proteins using hyperpolarized water, *J. Biomol. NMR*, 74(2–3), 161–  
472 171, doi:10.1007/s10858-020-00301-5, 2020.
- 473 Pérez, Y., Gairí, M., Pons, M. and Bernadó, P.: Structural characterization of the natively unfolded N-  
474 terminal domain of human c-Src kinase: insights into the role of phosphorylation of the unique domain.,  
475 *J. Mol. Biol.*, 391(1), 136–148, doi:10.1016/j.jmb.2009.06.018, 2009.
- 476 Piai, A., Caçada, E. O., Tarenzi, T., Grande, A. Del, Varadi, M., Tompa, P., Felli, I. C. and Pierattelli, R.: Just  
477 a flexible linker? the structural and dynamic properties of CBP-ID4 revealed by NMR spectroscopy,  
478 *Biophys. J.*, 110(2), 372–381, doi:10.1016/j.bpj.2015.11.3516, 2016.
- 479 Pontoriero, L., Schiavina, M., Murralli, M. G., Pierattelli, R. and Felli, I. C.: Monitoring the interaction of  $\alpha$ -  
480 synuclein with calcium ions through exclusively heteronuclear nuclear magnetic resonance experiments,  
481 *Angew. Chemie*, 132(42), 18696–18704, doi:10.1002/ange.202008079, 2020.
- 482 Robson, S., Arthanari, H., Hyberts, S. G. and Wagner, G.: Nonuniform sampling for NMR spectroscopy, in  
483 *Methods Enzymol.*, pp. 263–291., 2019.
- 484 Schiavina, M., Murralli, M. G., Pontoriero, L., Sainati, V., Kümmerle, R., Bermel, W., Pierattelli, R. and  
485 Felli, I. C.: Taking simultaneous snapshots of intrinsically disordered proteins in action, *Biophys. J.*,  
486 117(1), doi:10.1016/j.bpj.2019.05.017, 2019.
- 487 Schubert, M., Labudde, D., Oschkinat, H. and Schmieder, P.: A software tool for the prediction of Xaa-Pro  
488 peptide bond conformations in proteins based on <sup>13</sup>C chemical shift statistics, *J. Biomol. NMR*, 24(2),  
489 149–154, doi:10.1023/A:1020997118364, 2002.
- 490 Schuler, B., Lipman, E. A., Steinbach, P. J., Kumke, M. and Eaton, W. A.: Polyproline and the  
491 “spectroscopic ruler” revisited with single-molecule fluorescence., *Proc. Natl. Acad. Sci. U. S. A.*, 102(8),  
492 2754–9, doi:10.1073/pnas.0408164102, 2005.
- 493 Schütz, S. and Sprangers, R.: Methyl TROSY spectroscopy: A versatile NMR approach to study challenging  
494 biological systems, *Prog. Nucl. Magn. Reson. Spectrosc.*, 116, 56–84, doi:10.1016/j.pnmrs.2019.09.004,  
495 2020.
- 496 Shaka, A. J.; Barker, P. B.; Freeman, R.: Computer-optimized decoupling scheme for wideband  
497 applications and low-level operation, *J. Magn. Reson.*, 64(547), 552, 1985.
- 498 Shen, Y. and Bax, A.: Prediction of Xaa-Pro peptide bond conformation from sequence and chemical



- 499 shifts, *J. Biomol. NMR*, 46(3), 199–204, doi:10.1007/s10858-009-9395-y, 2010.
- 500 Szekely, O., Olsen, G. L., Felli, I. C. and Frydman, L.: High-resolution 2D NMR of disordered proteins  
501 enhanced by hyperpolarized water, , doi:10.1021/acs.analchem.8b00585, 2018.
- 502 Tamiola, K., Acar, B. and Mulder, F. A. A.: Sequence-specific random coil chemical shifts of intrinsically  
503 disordered proteins, *J. Am. Chem. Soc.*, 132(51), 18000–18003, doi:10.1021/ja105656t, 2010.
- 504 Thakur, A., Chandra, K., Dubey, A., D’Silva, P. and Atreya, H. S.: Rapid characterization of hydrogen  
505 exchange in proteins, *Angew. Chemie - Int. Ed.*, 52(9), 2440–2443, doi:10.1002/anie.201206828, 2013.
- 506 Theillet, F., Kalmar, L., Tompa, P., Han, K., Selenko, P., Dunker, A. K., Daughdrill, G. W. and Uversky, V. N.:  
507 The alphabet of intrinsic disorder, *Intrinsically Disord. Proteins*, 1(April), e24360, doi:10.4161/idp.24360,  
508 2014.
- 509 Tossavainen, H., Salovaara, S., Hellman, M., Ihalin, R. and Permi, P.: Dispersion from C $\alpha$  or NH: 4D  
510 experiments for backbone resonance assignment of intrinsically disordered proteins, *J. Biomol. NMR*,  
511 74(2–3), 147–159, doi:10.1007/s10858-020-00299-w, 2020.
- 512 Williamson, M. P.: The structure and function of proline-rich regions in proteins, *Biochem. J.*, 297(2),  
513 249–260, doi:10.1042/bj2970249, 1994.
- 514 Wong, L. E., Maier, J., Wienands, J., Becker, S. and Griesinger, C.: Sensitivity-enhanced four-dimensional  
515 amide–amide correlation NMR experiments for sequential assignment of proline-rich disordered  
516 proteins, *J. Am. Chem. Soc.*, 140(10), 3518–3522, doi:10.1021/jacs.8b00215, 2018.
- 517 Zhou, Z., Kümmerle, R., Qiu, X., Redwine, D., Cong, R., Taha, A., Baugh, D. and Winniford, B.: A new  
518 decoupling method for accurate quantification of polyethylene copolymer composition and triad  
519 sequence distribution with  $^{13}\text{C}$  NMR, *J. Magn. Reson.*, 187(2), 225–233, doi:10.1016/j.jmr.2007.05.005,  
520 2007.
- 521